Coordination Chemistry

DOI: 10.1002/anie.201203308

Paramagnetic NMR Shifts for Saddle-Shaped Five-Coordinate Iron(III) Porphyrin Complexes with Intermediate-Spin Structure**

*Ching-Chin Chen and Peter P.-Y. Chen**

In memory of Ru-Jen Cheng

The five-coordinate saddle-shaped iron(III) porphyrin complex, Fe(OETPP)Cl, has been identified as an admixed ($S = 3/2$, 5/2) spin electronic structure which can be used as a model for cytochrome c′ (OETPP = dianion of 2,3,7,8,12,13,17,18-octaethyl-5,10,15,20-tetraphenylporphyrin).[1] It has also been conjectured that a saddle deformation of the macrocycle results in a symmetry reduction, that is, a C_{2v} local symmetry, to raise the $d_{x^2-y^2}$ orbital energy by spatial mixing of the $d_{x^2-y^2}$ and d_{z^2} orbitals as shown by early spin-restricted ZINDO calculations.[2] Nevertheless, the definite composition, which is a mixture of the $S = 3/2$ and $S = 5/2$ spin states, still remains debatable.[1,3–5] When the axial ligand is changed from the Cl^- ion to a weaker ligand ClO_4^-, Fe(OETPP)ClO_4 recently has been characterized by a pure intermediate-spin state ($S = 3/2$) electronic structure.[4,6] Generally, the properties determined by Mössbauer spectroscopy, EPR and magnetic susceptibility measurements in the series of Fe(OETPP)X (X = Cl, Br, I, ClO_4) complexes are similar to planar five-coordinate iron(III) porphyrin complexes.[6–8] However, with careful examination of their paramagnetic NMR shifts, they exhibit a distinct difference in the ^{13}C NMR shifts at the *meso*-C position, which is important for analyzing the bonding interactions between a metal center and a porphyrin macrocycle.[7–10] For planar porphyrin ligands, such as high-spin FeTPPCl (or FeOEPCl), the *meso*-C signal appears at a downfield position of 500 ppm (or 380 ppm), and 368 ppm (or 246 ppm) for the admixed (5/2, 3/2) FeTPPClO_4 (or FeOEPClO_4), respectively (see Table 1; TPP = dianion of 5,10,15,20-tetraphenylporphyrin and OEP = dianion of 2,3,7,8,12,13,17,18-octaethylporphyrin).[11,12] These downfield shifts at the *meso*-C atoms have been attributed by Cheng et al. to interactions between the iron(III) d_{z^2} and the porphyrin a_{2u} orbitals.[13]

However, for saddled porphyrin ligands, considering the main skeleton of the macrocycle, the five-coordinate saddle-shaped Fe(OETPP)Cl has a local C_{2v} symmetry, which is lower than the C_{4v} symmetry of five-coordinate planar iron(III) porphyrin complexes. Theoretically, Fe(OETPP)Cl shall have similar bonding interactions as found for a C_{4v} symmetry. For example, the downfield shifts of 450 ppm for the *meso*-C atom, 525, 642 ppm for α-C atoms, and 973 ppm for β-C atoms of saddled Fe(OETPP)Cl are similar to those of planar five-coordinate iron(III) porphyrin complexes with admixed intermediate-spin states. The concept of d_{z^2}–a_{2u} interactions seems to apply to the case of Fe(OETPP)Cl for its downfield-shifted *meso*-C signal as well. Yet, in the case of Fe(OETPP)ClO_4, the *meso*-C signal was found at an unusual upfield position at −47 ppm.[14,15] The ^{13}C NMR signal for the *meso*-C atoms shifted upfield about 500 ppm as the axial ligand was changed from Cl^- to ClO_4^-. This shift is much larger than the average change of 132 ppm in planar five-coordinate iron(III) porphyrin complexes bearing the same axial ligands (see Table 1). This characteristic for the saddled porphyrin ligand implies that the d_{z^2}–a_{2u} interaction vanishes or is greatly weakened when the spin state changes to a pure $S = 3/2$ state. Normally, the disappearance of bonding interactions was found when the coordination number was altered as, for example, from a five- to a six-coordinate iron(III) porphyrin complex.[13] However, although the crystal structure of Fe(OETPP)ClO_4 still shows the five-coordinate saddled shape with a C_{2v} local symmetry which resembles Fe(OETPP)Cl, obviously the d_{z^2}–a_{2u} interaction is not sufficient to simultaneously interpret both saddled complexes.[6] This difference between Fe(OETPP)Cl and Fe(OETPP)ClO_4 has not been observed for five-coordinate planar iron(III)

Table 1: ^{13}C NMR chemical shifts δ_{obs} and (isotropic shifts, δ_{iso})[a] of five-coordinate complexes.

X	*meso*-C atom	α-C atom	β-C atom	*T* [K]
		Fe(TPP)X[7,11,12,14]		
Cl^-	500 (374)	1200 (1010)	1320 (1150)	303
ClO_4^-	368 (246)	438 (287)	634 (502)	302
		Fe(OEP)X[7]		
Cl^-	380 (282)	1163 (1015)	1224 (1081)	298
ClO_4^-	246 (148)	68 (−80)	398 (255)	298
		Fe(OETPP)X[7,15,16]		
Cl^-	456 (337)	525, 642 (378, 495)	973 (829)	298
ClO_4^-	−47(−166)	188 (41)	249 (105)	298

[a] $\delta_{iso} = \delta_{obs} - \delta_{dia}$; diamagnetic shifts were taken from the reference complexes of Zn(TPP), Zn(OEP), and Zn(OETPP).

[*] C.-C. Chen, Prof. P. P.-Y. Chen
Department of Chemistry, National Chung Hsing University
Taichung, Taiwan 402 (Republic of China)
E-mail: pychen@dragon.nchu.edu.tw

[**] We thank Prof. Ru-Jen Cheng for numerous valuable suggestions. This work was supported by funds from the Department of Chemistry, The National Center for High-Performance Computing, National Chung Hsing University, and by a grant from the National Science Council (NSC 100-2113-M-005-009-MY2).

Supporting information for this article is available on the WWW under http://dx.doi.org/10.1002/anie.201203308.

porphyrin complexes in similar spin states so far, but this change has been postulated because of the difference in the geometric structures.[7]

In this study, we employed density functional theory (DFT) calculations to correlate the Fe–porphyrin bonding interactions with calculated spin populations, including the total spin, the localized π spin, and the Fermi contact spin densities on the porphyrin macrocycle to elucidate these unexpected NMR data. By comparing the bonding characteristics of planar and saddled porphyrin ligands, DFT calculations have been carried out for both planar Fe(TPP or OEP)X and saddled Fe(OETPP)X (X = Cl^- and ClO_4^-) complexes with the ADF program. Molecular orbitals involving singly occupied α-spin $d_{x^2-y^2}$, d_{z^2}, and d_π orbitals are shown in Figure 1. The bonding strength between metal-d and porphyrin orbitals can be expressed by the effective orbital overlap, $\langle Fe^{3+}Cl\,|\,P^{-2}\rangle$, in terms of the product of the spatial overlap of orbitals between iron(III) chloride and porphyrin fragments, and their corresponding coefficients. To a first-order approximation, a negative value for the effective orbital overlap indicates the antibonding character of the d molecular orbitals (MOs) of iron(III) porphyrin complexes, which are given under the molecular orbital in Figure 1.

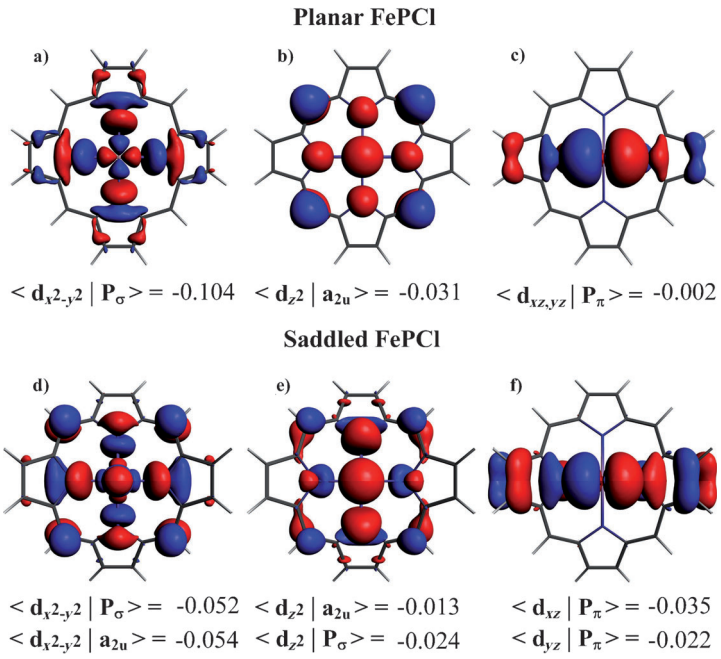

Figure 1. Selected α-set molecular orbitals based on spin-unrestricted calculations show the bonding interactions between iron occupied d and the porphyrin fragmental orbitals for planar FePCl ($S = 5/2$) complexes (a, b, c) and saddled FePCl ($S = 5/2$) (d, e, f). The effective orbital overlaps in space are also shown under each molecular orbital.

For high-spin ($S = 5/2$) planar iron(III) porphyrin complexes, as expected, the antibonding molecular orbital including the $d_{x^2-y^2}$ orbital and the porphyrin σ-type molecular orbital has nodal planes at the *meso*-C atoms (see Figure 1 a) and shows the strongest orbital interaction with $\langle d_{x^2-y^2}|P_\sigma\rangle = -0.104$. In Figure 1 b, the typical interaction between the d_{z^2} orbital and the porphyrin a_{2u} orbital shows $\langle d_{z^2}|P_{a_{2u}}\rangle = -0.031$ for the high-spin state and $\langle d_{z^2}|P_{a_{2u}}\rangle = -0.041$ for its intermediate-spin state, respectively, demonstrating a high preservation of the d_{z^2}–a_{2u} interactions after spin state changes. Other d orbital bonding interactions for $S = 5/2$ and $S = 3/2$ are collected in Tables S1 and S2 in the Supporting Information.

For saddled Fe(OETPP)Cl in the high-spin state, besides the bonding interaction between the metal $d_{x^2-y^2}$ orbital and the porphyrin σ-MO with $\langle d_{x^2-y^2}|P_\sigma\rangle = -0.052$, the new interaction between the d_{z^2} orbital and the porphyrin σ-type molecular orbital with $\langle d_{z^2}|P_\sigma\rangle = -0.024$ has to be considered (shown in Figure 1 e). Although the d_{z^2}–a_{2u} interaction still exists, the symmetry-allowed bonding interactions between $d_{x^2-y^2}$ and a_{2u} orbitals with $\langle d_{x^2-y^2}|P_{a_{2u}}\rangle = -0.054$ are four times stronger than the d_{z^2}–a_{2u} interactions with $\langle d_{z^2}|P_{a_{2u}}\rangle = -0.013$ (Figure 1 d and e). As for its $S = 3/2$ spin state, the $d_{x^2-y^2}$–a_{2u} and d_{z^2}–a_{2u} bonding interactions for the $S = 5/2$ spin state are similar in strength as shown in Tables S3 and S4. Importantly, the d_π–porphyrin(π) interactions with $\langle d_{xz},d_{yz}\,|\,P_\pi\rangle = -0.035$ and -0.022 are not only stronger than the $\langle d_{xz},d_{yz}\,|\,P_\pi\rangle = -0.002$ of the planar porphyrin, but also greater than its own d_{z^2}–a_{2u} interaction. The enhanced d_π–porphyrin(π) interaction induced by the saddled deformation may therefore increase the π-positive spin densities at the α-C atoms to sufficiently polarize the *meso*-C atoms which then show an upfield shift in the intermediate-spin state.

To clarify how these bonding interactions affect the chemical shifts, a detail analysis of the spin distribution on the macrocycle may reveal the relationship between decisive Fe–porphyrin bonding interactions and directions of ^{13}C NMR shifts for the significant carbon atoms of the macrocycle, and most importantly this analysis gives the chance to elucidate all components of the paramagnetic NMR shifts. The well-known shift terms of paramagnetic NMR shifts for $S = 5/2$ have been defined by the following Equations (1–7) for ^{13}C NMR shifts,[14,17,18]

$$\delta_{obs} = \delta_{dia} + \delta_{iso} \quad (1)$$

$$\delta_{iso} = \delta_{con} + \delta_{dip} = \delta_{con} + \delta_{dip}^{M.C.} + \delta_{dip}^{L.C.} \quad (2)$$

$$\delta_{con} = \frac{\mu_0 g_e^2 \mu_B^2 (S+1)}{9 k_B T} \rho_{\alpha\beta} \quad (3)$$

$$\delta_{dip}^{L.C.} = -\frac{28 g_e \mu_B D(2\Pi)}{9 g_N \beta_N (k_B T)^2} \rho^\pi = -1359\left(\frac{ppm}{cm^{-1}}\right) \times D \times \rho^\pi \quad (4)$$

$$\delta_{dip}^{M.C.} = -\frac{\mu_0}{4\pi} \frac{28 g_e^2 \mu_B^2 DG}{9(k_B T)^2}; = -0.1256\left(\frac{ppm}{cm^{-1}} cm^3\right) \times D \times G \quad (5)$$

$$G = \left[\frac{(3\cos^2\theta - 1)}{r^3}\right] / (10^{21}) cm^{-3} \quad (6)$$

$$\delta_{dip}^{L.C.} / \delta_{dip}^{M.C.} = \frac{4\pi}{\mu_0} \frac{2\Pi}{g_N \beta_N g_e \mu_B} \frac{\rho^\pi}{G} = 10820(cm^{-3}) \times (\rho^\pi / G) \quad (7)$$

where δ_{obs} is the observed NMR shift and δ_{dia} is a diamagnetic reference. The isotropic shift, δ_{iso}, includes two contributions known as the contact term, which originates from the spin

delocalization from metal-d orbitals through bonds into the nuclei of observed atoms, and two types of pseudo-contact dipolar terms, which are interactions through space including the metal-centered dipolar term $\left(\delta_{dip}^{M.C.}\right)$, that is, the interaction between the spin at the metal and any distant atom of the macrocycle, and the ligand-centered dipolar shift $\left(\delta_{dip}^{L.C.}\right)$, that is, the interaction between the observed carbon and its own π-spin densities. The contact shift (δ_{con}) is formulated by McConnell considering a normalization by 2*S*, where *S* denotes the total spin, $\rho_{\alpha\beta}$ refers to the unpaired spin density at zero distance from the nucleus, μ_0 is the vacuum permeability ($4\pi\times10^{-7}\,J^{-1}T^2m^3$), g_e is the free-electron *g*-factor (2.0023), μ_B is the Bohr magneton ($9.2740\times10^{-24}\,JT^{-1}$), *D* is the zero-field splitting, k_B is the Boltzmann constant, and *T* is the absolute temperature (298 K for this study).[19] In the two pseudo-contact terms, g_N is the *g*-factor of the nucleus (g_N for a ^{13}C atom is equal to 1.4048), β_N is the nuclear magneton ($5.0508\times10^{-27}\,JT^{-1}$), 2Π refers to the z component of the dipolar interaction for a unit of unpaired spins residing in a $2p_z$ carbon orbital (214 MHz), *G* is geometric factor, and ρ^π denotes the π-spin density at the observed carbon. These paramagnetic shifts can be simplified to relate only to the geometric factor, zero-field splitting, π-spin density, and Fermi contact spin density.

The net spin populations, π-spin densities, and Fermi contact spin populations on each symmetry-distinct atom type for a series of five-coordinate iron(III) porphyrin complexes in both high-spin and intermediate-spin states are summarized in Table 2. The separation of the π-spin density from the total spin densities at all interesting carbon atoms will facilely assist to analyze the bonding types. For example, the total net spin populations are almost equal to their corresponding π-spin densities at the *meso*-C atoms in both high-spin and intermediate-spin states for all planar five-coordinate iron(III) porphyrin complexes, ensuring that the d_{z^2}–a_{2u} bonding interaction is dominant relative to the spin delocalization at the *meso*-C atoms. By contrast, for saddled porphyrin ligands, Fe(OETPP)Cl and Fe(OETPP)ClO_4, the distinct difference is that the spin populations at the *meso*-C atom become negative in the intermediate-spin state. With the empty $d_{x^2-y^2}$ orbital, the spin transfer through $d_{x^2-y^2}$–a_{2u} interactions will not exist any longer, thus, the spin populations at the *meso*-C atoms shall reasonably decrease. Meanwhile, the greater d_π–porphyrin(π) orbital interaction is evidenced by high π-spin densities residing at α-C and β-C atoms relative to high-spin Fe(OETPP)Cl. Therefore, the *meso*-C atom can be polarized by adjacent α-C atoms. This is consistent with the observed highly alternant shifts of the ethyl group, that is, a signal at −66 ppm for the -CH_2- group and a downfield-shifted signal at +220 ppm for the -CH_3 group are found in the ^{13}C NMR spectrum which reflects hyperconjugation interactions induced by the β-C π-spin densities.[16] In addition, it is most important for the calculated π-spin density to evaluate the corresponding pseudo-contact shift.

The Fermi contact spin densities ($\rho_{\alpha\beta}$) of DFT spin-unrestricted calculations are able to qualitatively describe the direction of paramagnetic shifts to distinguish the determined ground state from many electronic structures.[20–23] This term is also successfully related to the isotropic shifts with neat linearity in many metalloporphyrin molecules, but it lacks a connection to the metal–porphyrin bonding interactions and completely neglects the pseudo-contact contributions because in the analyses of ^{13}C NMR data at α-, β-, and *meso*-C atoms, the contact shifts were thought to be more considerable than dipolar contributions.[24,25]

Table 2: Net spin populations and (π-spin densities, obtained from p_z orbitals which are reassigned the z axes to perpendicular to their sp^2 plane in calculations) and [the Fermi contact spin densities ($\rho_{\alpha\beta}$)] in the order of 10^{-3} on each symmetry-distinct atom type of five-coordinate iron(III) porphyrin complexes from unrestricted DFT calculations.

Symmetry, spin state	Fe	*meso*-C atom	α-C atom	β-C atom
		FeTPPCl		
C_{4v}, 5/2	4.0329	26.9(22.0) [3.4]	−0.8(−3.4)[5.8]	9.8(4.7)[6.4]
C_{4v}, 3/2	2.5809	15.7(18.8) [2.7]	−0.1(−1.3)[−2.7]	4.5(1.0)[0.0]
		FeTPPClO_4		
C_1, 3/2	2.6662	9.5(9.2)[1.6]	5.6(6.2)[−2.3]	14.7(13.2)[0.4]
		FeOEPCl		
C_{4v}, 5/2	4.0353	19.9(19.6)[2.7]	−0.2(−3.4)[5.5]	11.5(5.8)[6.0]
C_{4v}, 3/2	2.5920	13.1(12.1)[2.0]	1.2(1.2)[−2.4]	5.2(5.4)[0.4]
		FeOEPClO_4		
C_1, 3/2	2.6430	5.3(5.8)[0.9]	5.6(6.1)[−2.2]	19.1(17.5)[1.4]
		FeOETPPCl		
C_{2v}, 5/2	3.9560	24.0(21.6)[2.9]	9.2(3.1) [5.4]	15.7(10.4)[6.5]
C_{2v}, 3/2	2.6291	−6.2(−3.7)[−0.2]	6.4(2.8) [1.0]	5.9(5.3)[1.4]
		FeOETPPClO_4		
C_1, 3/2	2.6467	−9.0(−6.3)[−0.7]	10.8 (8.9)[1.0]	20.4(17.4)[2.4]

In our cases, the calculated Fermi contact spin populations ($\rho_{\alpha\beta}$) of α-, β-, and *meso*-C atoms are given in square brackets in Table 2. In high-spin Fe(TPP)Cl or Fe(OEP)Cl, the α- and β-C atoms show the highest Fermi contact spin densities. These densities are two times higher than that at the *meso*-C atom which has the highest π-spin density. In the correlation graph of the Fermi contact spin density versus (δ_{iso}−experimental $\delta_{dip}^{M.C.}$) the data of the *meso*-C atoms were excluded to show the effects induced by the highest π-spin densities in the chemical shifts (Figure S1). All data points are found very close to the regression curve, which implies that most atoms have negligible pseudo-contact shifts. Consideration of the *meso*-C atoms in this correlation diagram leads to data points which deviate from the regression curve and show a considerable deviation along the *x* axis. We regard these deviations as the ligand-centered dipolar contributions, which were calculated to be about −248 ppm in FeTPPCl and −209 ppm in FeOEPCl for the *meso*-C atoms. Accordingly, the corresponding contact shifts are determined from the slope to be about 601 and 473 ppm (Table S5). The zero-field splitting was derived to be about $8\,cm^{-1}$ by including the

calculated π-spin densities in the equation for the ligand-centered dipolar shift. This value is close to the values derived from variable-temperature ^{1}H NMR spectra.[26]

This successful division of the isotropic shifts shows that the ligand-centered dipolar shifts at the *meso*-C atoms in the high-spin state determines about 40% of the contact shifts in magnitude. The large contact shifts of α- and β-C atoms were mainly attributed to the effect of the unpaired spin in the $d_{x^2-y^2}$ orbital which is directly delocalized through the Fe–porphyrin σ-bonding MO distributions and penetrates into the corresponding nuclei. The less positive contact shifts of the *meso*-C atoms have been attributed to spin polarization from highly positive π-spin densities to the electrons in the 1s orbital. In the calculations of intermediate-spin states, α- and β-C atoms shall presumably shift upfield without an unpaired existed spin in the $d_{x^2-y^2}$ orbital. The negative Fermi contact spin population at the α-C atom is ascribed to spin polarization by a π-spin density localized at the vicinal pyrrole-N, β-, and *meso*-C atoms. The −80 ppm of isotropic shifts at α-C atoms of Fe(OEP)ClO$_4$ can be explained by more $S = 3/2$ spin state mixed in Fe(OEP)ClO$_4$ than in Fe(TPP)ClO$_4$, which is in accord with temperature-dependent magnetic susceptibility data.[27] In these examples of five-coordinate iron(III) porphyrin complexes, the ^{13}C NMR shifts of the carbon atoms with certain π-spin densities have significant ligand-centered dipolar contributions.

Likewise, as for saddled systems, the calculated Fermi contact spin densities of the α-, β-, and *meso*-C atoms in high-spin Fe(OETPP)Cl are all positive and truly reflect the relative magnitude of the isotropic shifts. As expected, the *meso*-C atoms of $S = 3/2$ Fe(OETPP)Cl or Fe(OETPP)ClO$_4$ display negative Fermi contact densities and further support the d_π–P(π) interaction which is greater than the d_{z^2}–a_{2u} interaction in pure intermediate-spin Fe(OETPP)ClO$_4$ (P = dianion of porphyrin with planar or saddle shape). Because of the lack of experimental $\delta_{dip}^{M.C.}$ data, the isotropic shifts were directly related to the Fermi contact spin densities. In the correlation plot, only the data of the α- and β-C atoms cause a considerable *x*-axis deviation relative to the regression curve, for which data from the α- and β-C atoms were excluded (see Figure 2).

The pseudo-contact shifts for α- and β-C atoms are about −100 and −300 ppm, respectively, and their corresponding contact shifts are around 178 and 416 ppm as estimated from the slope of the correlation graph. The ratio of the relative magnitudes between $\delta_{dip}^{L.C.}$ and $\delta_{dip}^{M.C.}$, namely $[(\rho^\pi/G) \times 10\,820]$, display their ligand-centered dipolar shifts are about 19 times higher than metal-centered dipolar shifts at the β-C and about three times for the α-C atoms. On the basis of these data, their corresponding ligand-centered dipolar shifts are presumably greater than the *x*-axis deviation mainly because of the mutually opposite signs of these two dipolar terms. Their dipolar contributions can be separated to calculate the zero-field splittings of 87 and 104 cm^{-1} from the data for the β-C and α-C atoms, respectively, based on the pseudo-contact equation for the $S = 3/2$ spin state (see the text in the Supporting Information). These two values show a small difference in the calculated metal-centered dipolar shifts for all atoms and a gap of 25–68 ppm in the ligand-centered

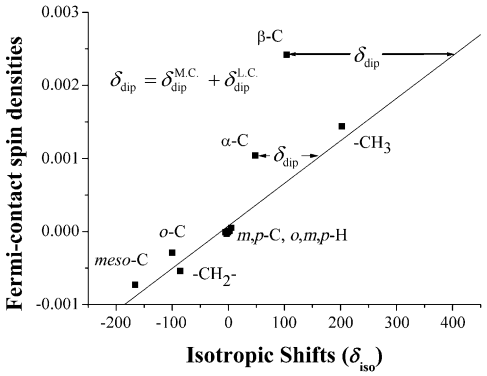

Figure 2. Correlation between the calculated Fermi contact spin densities at each symmetry-distinct atom type and the experimental isotropic shifts of Fe(OETPP)ClO$_4$ with a slope of 5.81×10^{-6} au ppm^{-1}, $R^2 = 0.942$ (excluding the data of α- and β-C atoms).

contributions for α-, β-, and *meso*-C atoms. The complete data concerning experimental geometric factors, ^{1}H NMR, calculated metal-centered dipolar shifts, and contact shifts obtained from detailed NMR analysis of Fe(OETPP)ClO$_4$ are collected in Table S6. In the case of intermediate-spin Fe(OETPP)ClO$_4$, the contribution of the ligand-centered dipolar shifts to those carbon atoms with high π-spin densities becomes significant for the total chemical shifts. Although the extent of the calculated ligand-centered dipolar shifts for α- and β-C atoms can be up to 80–90% of the corresponding contact shifts, ligand-centered dipolar shifts can also have the opposite sign which eventually leads to a mutual cancellation in the paramagnetic shifts. Thus, the small range of chemical shifts for Fe(OETPP)ClO$_4$ with $S = 3/2$ is completely understood.

In summary, the unrestricted DFT-based calculation presents explicit results in handling spin polarization for many open-shell metalloporphyrins. In our study, the compelling correlation between theoretical calculations and NMR spectroscopy of paramagnetic molecules is successfully inspected by MO bonding interactions and analyses of different spin populations. It is worth to mention at this point that the downfield shifts of *meso*-C atoms for all $S = 5/2$ five-coordinate iron(III) porphyrin complexes may not only be due the d_{z^2}–a_{2u} interaction. Herein, we have shown that the unpaired spin in the $d_{x^2-y^2}$ orbital, which has been seen as the conventional σ-type orbital, is also able to transfer its spin to the porphyrin macrocycle through $d_{x^2-y^2}$–a_{2u} bonding under saddled deformation. In the cases of Fe(OETPP)Cl and Fe(OETPP)ClO$_4$, this $d_{x^2-y^2}$–a_{2u} bonding interaction plays an important role in adjusting spin delocalization within the metal–porphyrin complex as a spin-switch at *meso*-C atoms, and interestingly, a series of the synthetic monoimidazole Fe^{III}(OETPP) complexes with intermediate-spin states have ^{13}C NMR spectra similar to Fe(OETPP)ClO$_4$,[16] which can be rationalized by the same bonding interactions. However, although the $d_{x^2-y^2}$–a_{2u} interaction has been found in six-coordinate saddled Mn^{III} or Fe^{III} porphyrin complexes, their $d_{x^2-y^2}$ orbitals are all empty and thus it is difficult to evaluate their influence by NMR spectroscopy.[20,21] The most important conclusion that can be drawn from the above results is to

disclose the trend in the antibonding strength for saddled five-coordinate porphyrin complexes: $d_{x^2-y^2}$–$a_{2u} > d_{\pi}$–porphyrin(π) > d_{z^2}–a_{2u}, which is the key reason for the conversion of spin populations at *meso*-C atoms to be negative in the intermediate-spin state.

Another important conclusion from the preceding discussions is that the paramagnetic NMR shifts can be successfully divided into their component contributions based on the calculated Fermi contact spin and π-spin densities. As the major part of our continuing research interest, here we have demonstrated that the symmetry-controlled bonding interaction may play an important role in adjusting spin densities on the macrocycle of natural hemoproteins.

Received: April 30, 2012
Revised: July 31, 2012
Published online: August 21, 2012

Keywords: density functional calculations · electronic structure · iron · NMR spectroscopy · porphyrins

[1] R. J. Cheng, P. Y. Chen, P. R. Gau, C. C. Chen, S. M. Peng, *J. Am. Chem. Soc.* **1997**, *119*, 2563 – 2569.
[2] R. J. Cheng, P. Y. Chen, *Chem. Eur. J.* **1999**, *5*, 1708 – 1715.
[3] V. Schünemann, M. Gerdan, A. X. Trautwein, N. Haoudi, D. Mandon, J. Fischer, R. Weiss, A. Tabard, R. Guilard, *Angew. Chem.* **1999**, *111*, 3376 – 3379; *Angew. Chem. Int. Ed.* **1999**, *38*, 3181 – 3183.
[4] M. Nakamura, *Coord. Chem. Rev.* **2006**, *250*, 2271 – 2294.
[5] R. Weiss, A. Gold, J. Terner, *Chem. Rev.* **2006**, *106*, 2550 – 2579.
[6] K. M. Barkigia, M. W. Renner, J. Fajer, *J. Porphyrins Phthalocyanines* **2001**, *5*, 415 – 418.
[7] M. Nakamura in *Coordination Chemistry Research Progress* (Eds.: T. W. Cartere, K. S. Verley), Nova Science Publishers, New York, **2008**, pp. 13 – 70.
[8] M. Nakamura, T. Ikeue, Y. Ohgo, M. Takahashi, M. Takeda, *Chem. Commun.* **2002**, 1198 – 1199.
[9] A. Hoshino, Y. Ohgo, M. Nakamura, *Inorg. Chem.* **2005**, *44*, 7333 – 7344.
[10] A. Ikezaki, M. Nakamura, R. J. Cheng, *Chem. Lett.* **2006**, *35*, 156 – 157.
[11] H. M. Goff, E. T. Shimomura, M. A. Phillippi, *Inorg. Chem.* **1983**, *22*, 66 – 71.
[12] G. E. Toney, A. Gold, J. Savrin, L. W. Ter Haar, R. Sangaiah, W. E. Hatfield, *Inorg. Chem.* **1984**, *23*, 4350 – 4352.
[13] R. J. Cheng, P. Y. Chen, T. Lovell, T. Q. Liu, L. Noodleman, D. A. Case, *J. Am. Chem. Soc.* **2003**, *125*, 6774 – 6783.
[14] J. Mispelter, M. Momenteau, J.-M. Lohoste, *J. Chem. Soc. Dalton Trans.* **1981**, 1729 – 1734.
[15] T. Sakai, Y. Ohgo, T. Ikeue, M. Takahashi, M. Takeda, M. Nakamura, *J. Am. Chem. Soc.* **2003**, *125*, 13028 – 13029.
[16] A. Ikezaki, M. Takahashi, M. Nakamura, *Angew. Chem.* **2009**, *121*, 6418 – 6421; *Angew. Chem. Int. Ed.* **2009**, *48*, 6300 – 6303.
[17] I. Bertini, C. Luchinat, G. Parigi, *Solution NMR of Paramagnetic Molecules*, Elsevier, Amsterdam, **2001**.
[18] J. Mispelter, M. Momenteau, J. M. Lohoste in *Biological Magnetic Resonance*, *Vol. 12* (Eds.: L. J. Berliner, J. Reuben), Plenum, New York, **1993**.
[19] H. M. McConnell, D. B. Chesnut, *J. Chem. Phys.* **1958**, *28*, 107 – 117.
[20] R. J. Cheng, Y. K. Wang, P. Y. Chen, Y. P. Han, C. C. Chang, *Chem. Commun.* **2005**, 1312 – 1314.
[21] R. J. Cheng, S. H. Chang, K. C. Hung, *Inorg. Chem.* **2007**, *46*, 1948 – 1950.
[22] R. J. Cheng, C. W. Chao, Y. P. Han, Y. C. Chen, C. H. Ting, *Chem. Commun.* **2009**, 2180 – 2182.
[23] R. J. Cheng, C. H. Lee, C. W. Chao, *Chem. Commun.* **2009**, 2526 – 2528.
[24] J. H. Mao, Y. Zhang, E. Oldfield, *J. Am. Chem. Soc.* **2002**, *124*, 13911 – 13920.
[25] Y. Ling, Y. Zhang, *J. Am. Chem. Soc.* **2009**, *131*, 6386 – 6388.
[26] F. A. Walker, G. La Mar, *Ann. N. Y. Acad. Sci.* **1973**, *206*, 328 – 348.
[27] S. Mitra in *Iron porphyrin*, *Part II* (Eds.: A. B. P. Lever, H. B. Gray), Addison-Wesley, Reading, MA, **1983**.

